Journal of Electrotechnology, Electrical Engineering and Management (2024)
Clausius Scientific Press, Canada
DOI: 10.23977/jeeem.2024.070307
ISSN 2560-6697 Vol. 7 Num. 3

Analysis of electric field defect problems based on IGBT modules

Zikang He[1], Fei Wu[2,*]

[1]*School of Electrical Engineering, Tongda College of Nanjing University of Posts and Telecommunications, Yangzhou, 225100, China*
[2]*School of Electrical Engineering, Xinjiang University, Urumqi, 830049, China*
[*]*Corresponding author: 13461186266@163.com*

Keywords: Insulated gate bipolar transistor (IGBT), electrostatic field simulation, triple junction, defect problem

Abstract: With the development of new power systems, IGBT has been more widely used in rail transit, new energy vehicles, photovoltaic power generation and other fields. The high efficiency and reliability of electrical insulation have received widespread attention. In this paper, in order to solve the problem of defects in the use of IGBT chips in the electrostatic field, the IGBT electrostatic field simulation model was constructed in COMSOL through the finite element method, and the results of different defects were explored through the electric field distributions presented in the simulation results. It is concluded that voids, bubbles, and metal protrusion defects all have an effect on the electric field distribution at the triple bonding point, and the field strength inside the defects is greater. Meanwhile, the corresponding data base is also provided for the device design of IGBT.

1. Introduction

In 1957, General Electric successfully developed the world's first thyristor, whose superior electrical and control performance quickly led to its replacement by mercury rectifiers. In the late 1980s, the insulated gate bipolar transistor (IGBT) was introduced as a new type of power semiconductor[1], combining the advantages of the bipolar junction transistor (BJT) and the metal-oxide-semiconductor field-effect transistor (MOSFET) with Low on-state pressure drop, High current density, High withstand voltage characteristics, but also with low drive power, fast switching speeds and High withstand voltage characteristics. With the continuous advancement of new power systems, IGBTs play a crucial role in computers, communications, aerospace, rail transport and other fields. In addition, the evolution of power electronic devices has had a decisive impact on the development of power electronics. With the development of IGBT, although the welding type power module has a long history of research and development and mature technology, its internal defect problem can still not be ignored. For example, at the three bonding points[2][3] (Ceramic layer, upper copper layer, silicone gel[4][5]) is prone to produce bubbles, so that the bubble at the larger field strength. Therefore the defect problem inside the IGBT cannot be ignored. Combined with the current research articles, the study of these defect problems are also indicated. By taking the local onset voltage as the control

quantity, they obtained the corresponding electric field distribution and the onset field strength of partial discharge with the help of simulation software, and analysed the influence law of the electrical parameters of the nonlinear field grading(NFG) coating material on the electric field at the three bonding points of the direct-bond copper(DBC) substrate. The electrical parameters of the NFG coating material are analysed to determine the influence of the electric field on the DBC substrate at the three bonding points, and NFG parameter setting suggestions are given, which provides data for improving the design of the local electric field of the DBC substrate. At present, there is no systematic research on the defect problem of IGBT electrostatic field[6-8].

On the basis of the aforementioned research background, this paper provides an in-depth discussion of the structure of welded IGBT modules and their research progress, [9][10] as well as an exhaustive analysis of the defects and difficulties in the calculation of their internal electric fields. We focus on the common metal protrusions during the welding of bonding wires, the formation of bubbles at the triple bonding point, and the appearance of voids in the grooves of the DBC ceramic layer. Using COMSOL software, we constructed an electric field simulation model of the IGBT module and adjusted the relevant parameters to determine the final electric field distribution. By comparing with the base model, we elucidated the specific impact of these defect problems on the performance of the IGBT module, thus providing solid theoretical support for the design of IGBT devices.

2. Experimental platform and method

2.1 Basic structure of an IGBT module

The core part of the IGBT consists of two diode chips (FWD) and two IGBT chips[11]. The DBC lower copper layer in the module is soldered to the copper substrate by means of the lower solder layer. The IGBT chip and the diode chip are engraved on the DBC upper copper layer in a soldering manner using the upper solder layer and are connected by means of bonding wires, thus constituting the power circuit of the circuit. In order to increase the load current of the IGBT module and to reduce the impedance of the electrical connections, several bonding wires are connected in parallel. The upper and lower copper layers of the DBC and the ceramic layer form the mechanical support structure of the IGBT module, which not only insulates the upper and lower parts electrically, but also conducts the heat inside the module to the copper substrate. Through the above welding method, the IGBT module forms a stable internal structure. It also facilitates heat transfer between adjacent structures. The module package is filled with silicone material, which is conducive to the formation of good thermal conductivity, insulation and vibration damping. Finally, the simulation model is constructed through COMSOL simulation software[12], as shown in Fig.2.

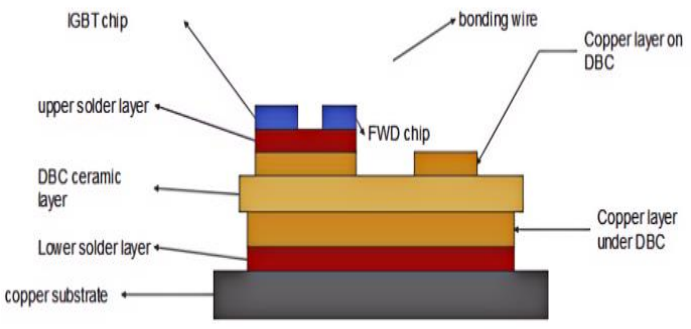

Figure 1: Internal structure of IGBT module

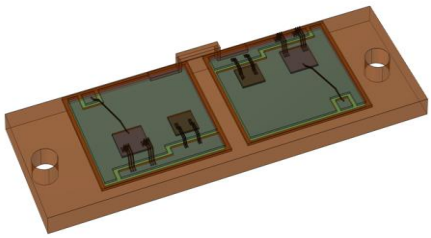

Figure 2: IGBT simulation model

2.2 Finite element model of IGBT power module [13][14]

Table 1: Resulting dimensions of each part of the IGBT module [15]

Structure	Material	Length / mm	Width / mm	Height / mm
diode chips	Silicon	5.55	5.55	0.15
IGBT chip	Silicon	6.90	6.90	0.15
Diode chip solder layer	96.5Sn3.5Ag	5.55	5.55	0.12
IGBT chip solder layer	96.5Sn3.5Ag	6.90	6.90	0.12
Copper layer on DBC	Cu	28.50	25.80	0.30
DBC ceramic layer	Al_2O_3	30.65	28.00	0.38
Copper layer under DBC	Cu	28.50	25.80	0.30
DBC solder layer	96.5Sn3.5Ag	28.50	25.80	0.12
Copper substrate	Cu	91.40	31.40	2.80

Table 1 describes the material dimensions of each layer of the IGBT module simulation model (see Fig. 2).

2.3 Establishment of electric field boundary constraints

Fig.3 shows a schematic diagram of the electric field boundary condition setting for the IGBT module. In the electric field study, the current is input to the IGBT module when the current passes through the bonding wires of the module. The lower part of the upper copper layer on the left side is grounded and the bonding wire connected to the lower part, the upper surface of the IGBT chip and the upper surface of the diode chip are grounded, and the copper substrate is similarly grounded. The right upper copper layer is connected to the terminals and the gate conducts.

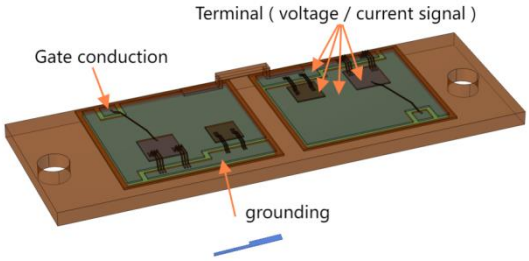

Figure 3: Electric field boundary conditions

3. Results

3.1 Simulation analysis of IGBT electric field

3.1.1 Initial model simulation results

The IGBT electrostatic field potential obtained based on COMSOL calculation is shown in Fig.4. The results show that the potential gradually decreases from the surface of the upper copper layer upward encapsulation insulation, the highest potential reaches 5.0×10^{6} V, and gradually decreases from the IGBT chip and diode chip to the surrounding edges. Due to the different dielectric constants between layers, the potential spans from the upper copper layer to the DBC ceramic layer.

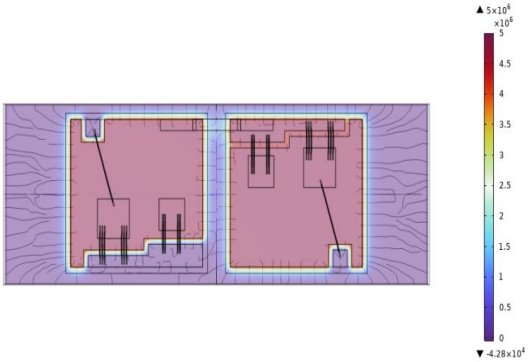

Figure 4: Initial model of electric potential

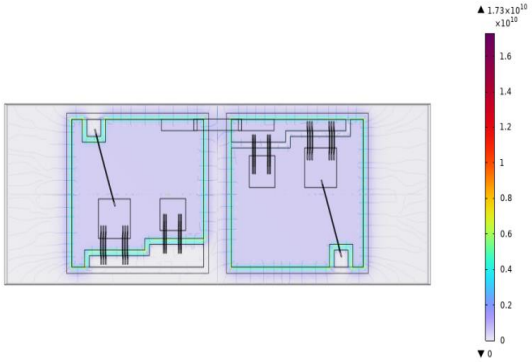

Figure 5: Initial model of electric field mode

The distribution of electric field modes of the IGBT electrostatic field obtained based on COMSOL calculations is shown in Fig.5. The results show that there are unstable electric field modes distributed in the trench of the grounded end of the upper copper layer in the range of 1.0×10^{6} — 0.4×10^{6} V/M, especially between the upper copper layer, ceramic layer and organosilicon gel, which is the most prominent distribution of unstable electric field modes. The electric field modes on the surface of the upper copper layer and the surface of the chip are lower, at 0.2×10^{6} V/M.

3.1.2 Cavity-defect simulation results

Radius size of cylindrical cavity is shown in Table 2. The potential distribution and electric field modes of IGBT cavities obtained based on COMSOL calculations are shown in Fig.6. The results show that in the potential distribution, when a cavity appears in the trench, the existence of the cavity affects the height of the surrounding potential, and along with the increase in the radius of the cavity, the scope of its influence gradually becomes larger, around the outside of the cavity, the potential decreases the fastest, and the potential inside the cavity is almost zero.

In the electric field mode distribution, the increase of the cavity leads to the decrease of the electric field mode of the whole IGBT module, and the overall decrease of the IGBT module is relatively slow between the radius of 0.1mm-0.3mm; when the radius becomes 0.4mm from 0.3mm, the decrease of the electric field mode between the grooves is more obvious; when the radius becomes 0.5mm, the overall electric field mode of the IGBT is almost zero. When the radius becomes 0.5mm, the overall electric field mode of IGBT is almost zero. However, no matter how the radius of the cavity changes, there is a large distribution of uneven electric field mode in the cavity attachment, and its value starts to decrease from 3.5×10^{10} V/M.

Table 2: Radius size of cylindrical cavity

Radius size (mm)	R_1	R_2	R_3	R_4	R_5
Cylindrical hollow	**0.1**	**0.2**	**0.3**	**0.4**	**0.5**

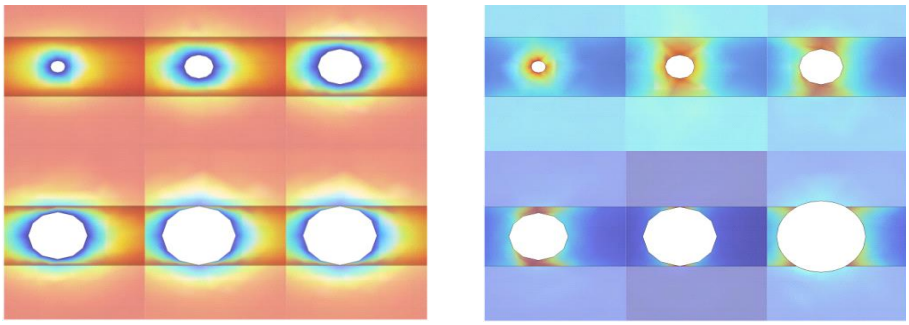

(a) (b)

Figure 6: Distribution of potential (a) and electric field in the cavity (b)

The local description of the potential and electric field distribution of the IGBT module in the ideal state is obtained by COMSOL calculation and local amplification, as shown in Fig.7. Before there is no cavity, the potential distribution in the gully is relatively uniform; in the electric field distribution, the gully will have an electric field strength that is not uniformly distributed and can be up to 0.8×10^{7} V/M.

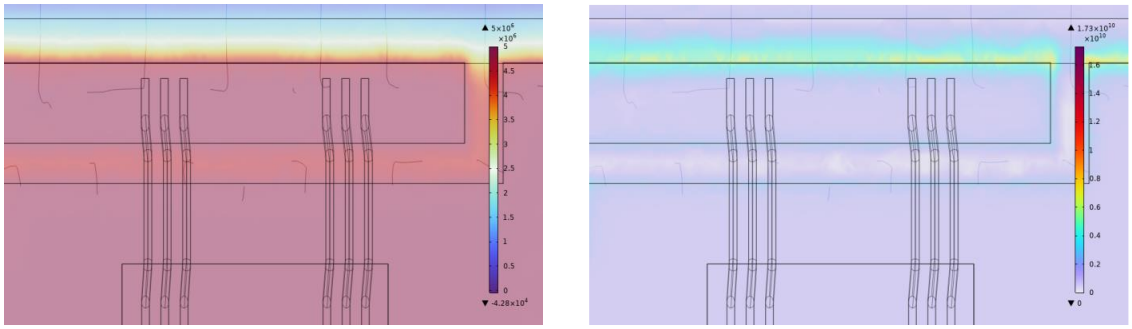

(a) (b)

Figure 7: Local potential (a) and local electric (b) field distribution in ideal state

3.1.3 Bubble-defect simulation results

Bubble size is shown in Table 3. The IGBT bubble potential distribution and electric field modes obtained based on COMSOL calculations are shown in Fig.8 and Fig.9. The results show that in the potential distribution diagram, the presence of bubbles in the trench seam, the potential distribution of the IGBT module is less affected by the bubble, only in the outer edge of the bubble there will be a more pronounced drop in potential. And along with the bubble becomes bigger, the influence by the bubble is increasing trend.

In the electric field mode distribution graph compared with the initial model, when there is a small bubble in the IGBT module, the electric field mode will be reduced especially obviously, and its electric field mode is almost 0. There will be an uneven distribution of electric field around the outer surface of the bubble, and from the outer surface of the bubble towards the outer surface of the decreasing trend. However, as the bubble becomes larger, the overall electric field mode of the IGBT module gradually increases, but is not larger than the initial model, and the electric field around the bubble gradually becomes uniformly distributed, and shows a uniform trend of decreasing outward.

Table 3: Bubble size

Radius size (mm)	R_1	R_2	R_3	R_4	R_5	R_6
bubble	**0.05**	**0.08**	**0.11**	**0.14**	**0.17**	**0.20**

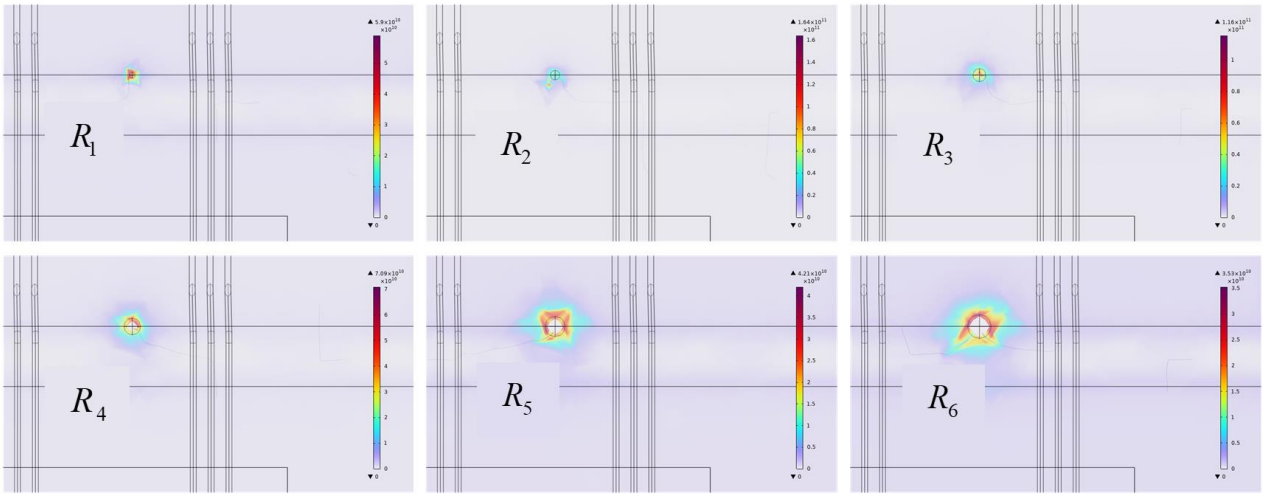

Figure 8: Electric field distribution map of bubble defect

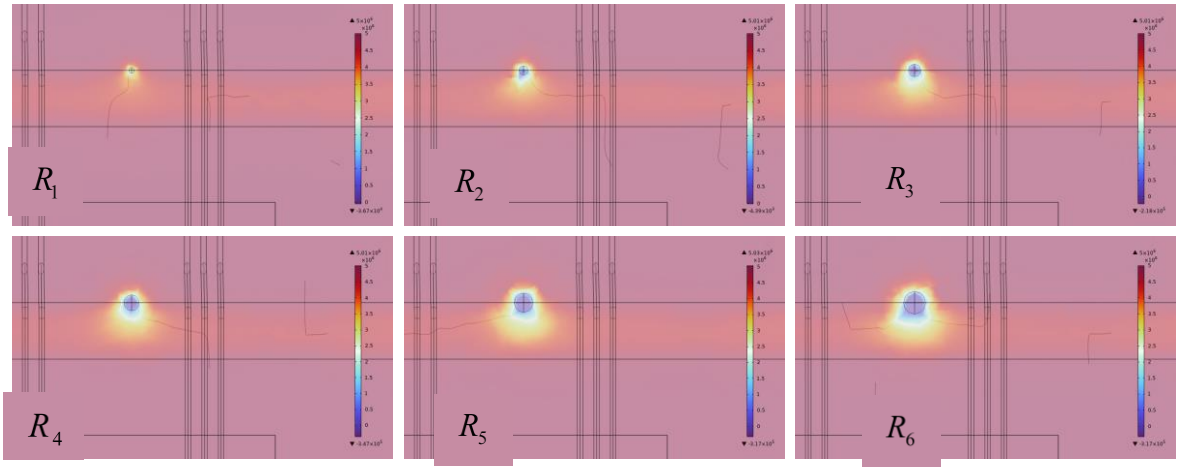

Figure 9: Electric potential mode distribution of bubble defect

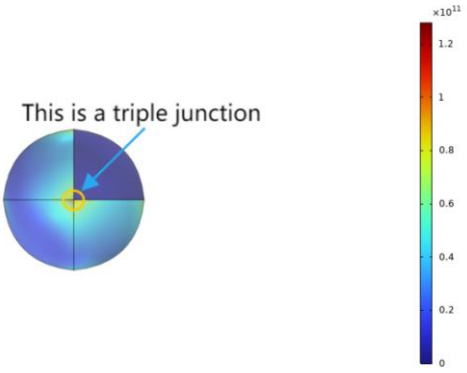

Figure 10: Bubble electric field diagram when the radius is R_4

According to Fig.10, it can be concluded that after the appearance of bubbles at the triple bonding

point, higher voltages will converge here, with a value of up to 0.8×10^{11} V/M, which will have a greater impact on the use of the IGBT module, leading to a decrease in the stability of its performance and a reduction in its service life.

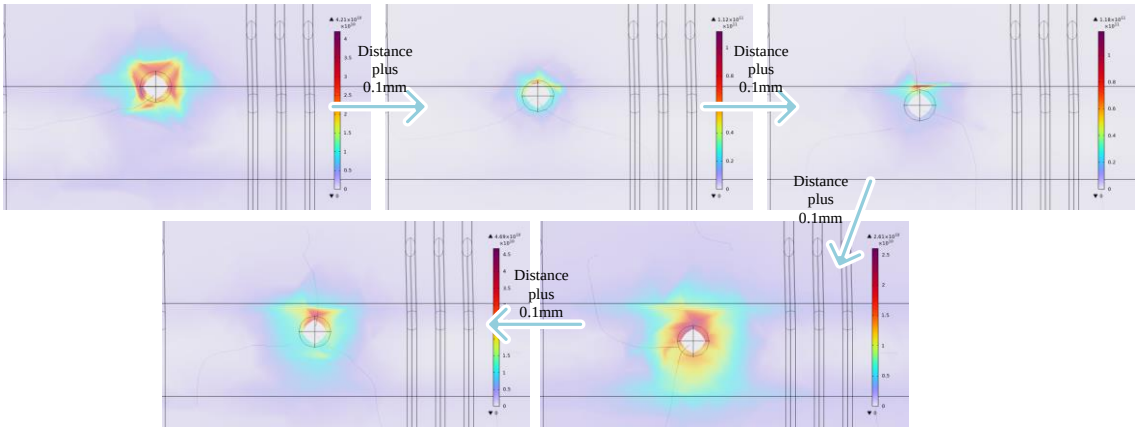

Figure 11: Radius is the electric field diagram of R_5 bubble position.

The electric field at the distance of the IGBT bubble position from the triple bonding point obtained based on COMSOL calculations is shown in Fig.11. We adopted R^4 as the quantification and the distance from the bubble to the triple bonding point as the variable. The results show that when the distance from the bubble to the triple bonding point belongs to the enhancement in a certain range, when the distance gradually reaches the centre of the gully, the strength of the electric field near the bubble gradually decreases again, but it is always higher than the strength of the electric field in the initial model of the electric field in Fig.5.

3.1.4 Metal protrusion-defect simulation results

Considering that the size of the metal protrusions and the size of the position located at the end of the bonding line will have more or less influence on the distribution of its electric field, a method of classifying and comparing the metal protrusions has been adopted to make the results of the size of the metal protrusions and the distance of their positions in turn.

Here a square metal is used to represent the metal protrusions, the size of its square side lengths as indicated in Table 4.

Table 4: The size of the side length of the metal protrusion

Side length (mm)	A_1	A_2	A_3	A_4	A_5	A_6
metal protrusion	**0.1**	**0.2**	**0.3**	**0.4**	**0.5**	**0.6**

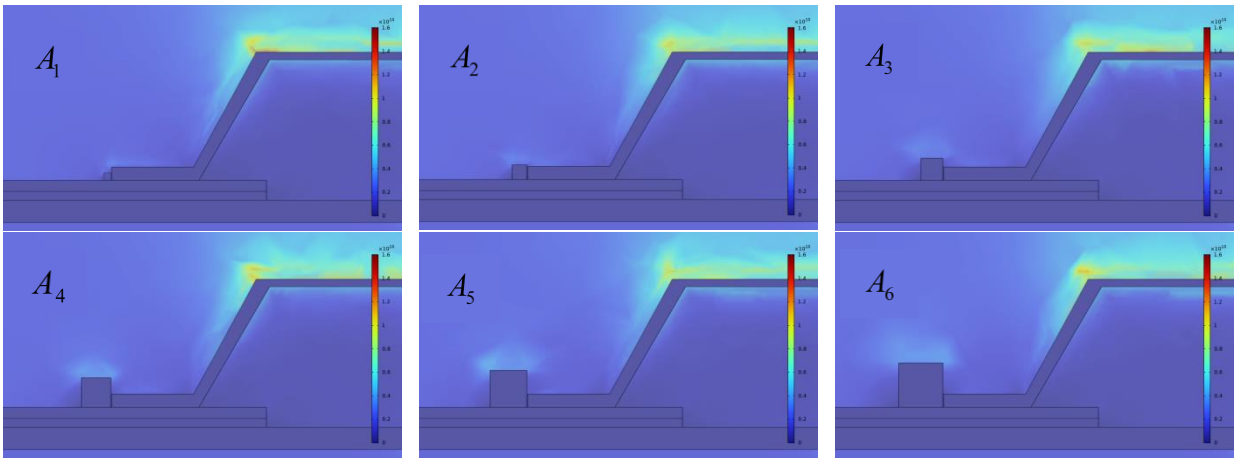

Figure 12: Electric field distribution of metal protrusions

The electric field mode distribution of IGBT metal protrusions obtained based on COMSOL calculations is shown in Fig.12. The results show that when the metal protrusion appears at the welding place due to improper welding of the bonding wire, the voltage will gather on the upper surface of the metal protrusion, and as the metal protrusion gets bigger, the voltage on the upper surface becomes more and more obvious, with the value size between 0.5×10^{10} -0.3×10^{10} V/M, and the distribution range of which increases accordingly. When the metal protrusion is smaller than the size of the bonding wire weld, it leads to the existence of voltage on the upper surface of the bonding wire weld, and when the metal protrusion increases, the voltage on the upper surface gradually becomes smaller.

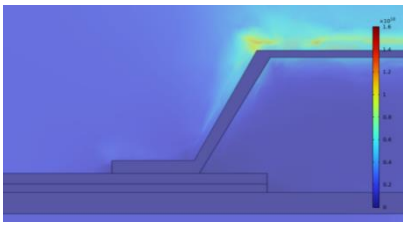

Figure 13: Electric field distribution of ideal model

The simulation results of the model in its ideal state are shown in Fig.13. It can be seen that when there is no metal protrusion, the electric field at the contact end of the bonding wire and chip is very small. Its service life will be longer and its performance more stable.

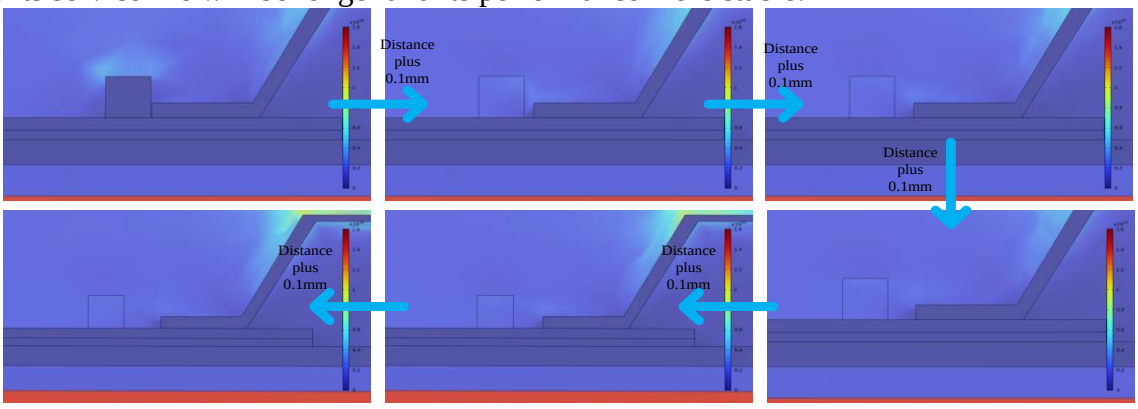

Figure 14: Variation of electric field with position of metal protrusion

In order to be able to observe more dramatically the change in the electric field with change in

position of the metal protrusions, a square metal with side length A_3 was used for the calculations shown in Fig.14. The results show that the electric field incident around the metal protrusion becomes less and less pronounced as the position changes, while the electric field incident on the bonding wire gradually extends towards the port.

3.2 Analysis of experimental results

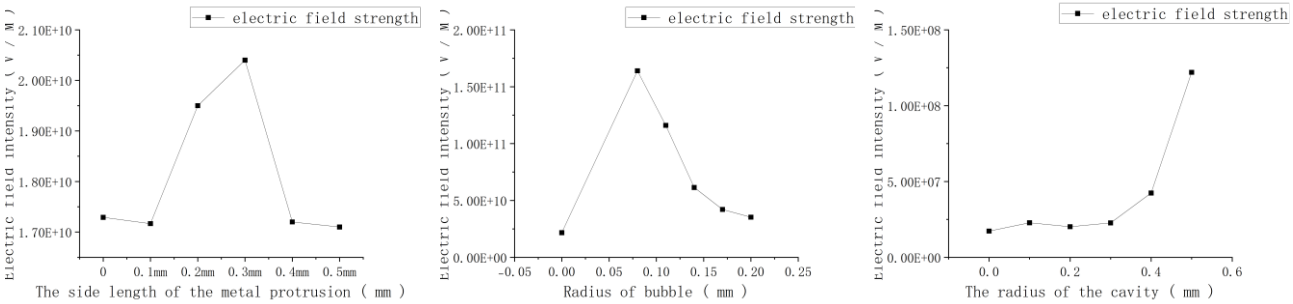

Figure 15: Dot plot of radius of metallic protrusions (a) radius of bubbles (b) radius of voids (c) versus electric field strength respectively

The intricate COMSOL simulations, as exemplified in Fig.15 (a), vividly depict the scenario where the metallic protrusion assumes a rectangular shape. In this context, the IGBT module's comprehensive electric field intensity undergoes a marked amplification when confronted with metallic protrusions stemming from excessive welding during the assembly process. Notably, as the protrusion's length and width vary within the range of 0.1mm to 0.4mm, a pronounced escalation in electric field intensity is observed, portending potential adverse implications for the IGBT module's operational integrity and longevity, ultimately threatening its overall performance.

As depicted in Fig.15 (b), the comprehensive COMSOL calculation results are consolidated, showcasing the scenario where the absence of a bubble within the IGBT module results in an electric field strength of 2.17×10^{10} V/M. Furthermore, upon the emergence of a bubble at the triple bonding point, an inverse correlation between the bubble's size and the electric field strength becomes evident, as can be discerned from the figure. This observation underscores that the presence of a smaller bubble exerts the most pronounced influence on the IGBT module, underscoring its severity.

As illustrated in Fig.15 (c), comprehensive COMSOL calculation results have been amalgamated. In the absence of a cavity within the IGBT module, the electric field strength is measured to be 1.73×10^{7} V/M. Conversely, in the presence of a cavity, the figure reveals that the cavity's radius, ranging from 0.1mm to 0.3mm, exerts minimal influence on the electric field strength. However, as the radius surpasses 0.3mm, the electric field strength gradually intensifies. Additionally, it underscores that the presence of voids within a specific range does not significantly affect the IGBT module, implying that prompt repair, once detected, will not compromise its performance. Nonetheless, when the cavity enlarges to a critical point, its impact on the IGBT module becomes irreparable.

4. Analysis of results

In this paper, we constructed a welded IGBT module through COMSOL simulation software, sorted out the electric field defect problem of the IGBT module, and analysed several more common situations in the defect problem.

As the radius of the cavity increases, the potential of the IGBT module does not change

significantly, but only around the cavity has a greater impact. Electric field mode distribution: the overall electric field of the IGBT module does not change significantly, but around the outside of the cavity will gather a higher electric field, and the outward trend is decreasing. As the radius of the cavity increases, the overall electric field of the IGBT is decreasing, and the change is more obvious. The change in the radius of the cavity and the electric field mode change is inversely proportional to the relationship.

When IGBT bubbles appear. Electric field mode distribution: A higher electric field will gather around the outside of the bubble, and as the bubble becomes larger, the electric field will become more uniform. When the bubble is small, the electric field mode is almost unchanged. As the bubble gets larger, the electric field mode increases, but not more than in the case of no bubble. The size of the bubble is directly proportional to the strength of the electric field mode.

When the IGBT module bonding wire welding is not standardised, resulting in metal protrusions, the potential distribution: the same as the ideal model potential distribution. Electric field distribution: the whole and the ideal state is almost unchanged, but the upper surface of the metal protrusion will gather voltage, and with the increase of the metal protrusion and increase. The size of the voltage on the upper surface is proportional to the size of the metal protrusion.

According to the analysis of the experimental results, it is concluded that among the defect problems of the IGBT module, the bubbles at the three bonding points have the most serious impact on it, followed by the metal protrusions appearing as a result of improperly welded bonding wires. Lastly, there is a cavity between the grooves, which is found and treated in time within a certain period of time and causes the least impact; however, when it cannot be found and treated in time, the impact caused by it is also unpredictable.

5. Conclusions

This paper analyses the defect problems on the electrostatic field model of IGBT module, but due to my limited level, some problems are still to be further studied and discovered. In this paper, the air bubbles at the three bonding points, the metal protrusions caused by improper welding bonding line and the voids between the grooves and other defects were studied.

(1) It is found that the defects such as air bubbles at the triple bonding point, metal protrusions caused by improperly welded bonding wires, and voids between the grooves of the IGBT module have a significant effect on the electric field strength and potential.

(2) The effect of air bubbles at the triple bonding point is the most serious, followed by metal protrusions, while the effect of voids between grooves is relatively small, but unpredictable if not dealt with in time.

(3) As IGBT as the core device in power electronics technology, the stability of its performance has a direct impact on the reliability and efficiency of new energy generation, industrial equipment and other fields, continuous improvement and innovation for its defect problems will have a greater role in the development of power electronics technology.

References

[1] Dai Chao, Chen Xiangrong. A review of research on packaging and insulation of silicon carbide IGBT power electronics [J]. Zhejiang Electric Power, 2019, 38(10):26-33.DOI:10.19585/j.zjdl.201910005.

[2] Wang Zhengdong, Luo Meng, Cheng Yonghong. A review on the failure mechanism of high-voltage high-power IGBTs and the research on high-temperature-resistant modified organosilicon potting materials[J]. High Voltage Technology, 2023, 49(04):1632-1644.DOI:10.13336/j.1003-6520.hve.20221925.

[3] Wen Teng. Calculation method and application research of transient electric field inside crimped IGBT devices[D]. North China Electric Power University (Beijing), 2022. DOI:10.27140/d.cnki.ghbbu.2022.000142.

[4] Yuan W.B. Research on key technology of condition monitoring and fault diagnosis of IGBT module [D]. Hefei

University of Technology, 2022. DOI:10.27101/d.cnki.ghfgu.2022.001510.
[5] Sun Junda. Analysis of internal electric field and insulation design of crimped IGBT devices[D]. North China Electric Power University (Beijing), 2017.
[6] Liu Zhaocheng, Cui Xiang, Li Xuebao, et al. A review of research on electric field calculation of insulation structure of high-voltage high-power IGBT devices[J]. Chinese Journal of Electrical Engineering, 2024, 44(01):214-231.DOI:10. 13334/j. 0258-8013.pcsee.223284.
[7] Li Wenyi, Wang Yalin, Yin Yi. A review of reliability studies on package insulation for high-voltage power modules[J]. Chinese Journal of Electrical Engineering, 2022, 42(14):5312-5326.DOI:10.13334/j.0258-8013.pcsee.210545.
[8] Zhou Z , Sha Y , Wei L ,et al.Thermal Stress Analysis of IGBT Module Based on ANSYS[J].Springer, Cham, 2022.DOI:10.1007/978-3-030-81007-8_30.
[9] Yin Zhihao, Yu Dianru, Zhu Jiafeng, et al. A review of IGBT power module package failure mechanisms and monitoring methods[J]. New Technology of Electrical Engineering, 2022, 41(08):51-70.
[10] Liu Renkuan, Li Hui, Yu Kai, et al. Analysis of package state monitoring method for soldered IGBT devices[J]. Electrotechnology, 2022, (15):71-78+82.DOI:10.19768/j.cnki.dgjs.2022.15.019.
[11] Zhou W.D. Electric-thermal-force coupling and failure analysis of IGBT modules [D]. South China University of Technology, 2016.
[12] Liu SJ, Wen Teng, Li XB, et al. Electric field transient characteristics in the package insulation structure of high-voltage high-power elastically crimped IGBT devices[J]. Journal of Electrotechnology, 2023, 38(23):6253-6265.DOI: 10.19595/j. cnki.1000-6753.tces.221474.
[13] Yue Yajing. Failure analysis and research on bonding wire of IGBT power module[D]. Tianjin University of Technology, 2019.
[14] Waheed A , Rehman S U , Alsaif F ,et al.Hybrid multimodule DC–DC converters accelerated by wide bandgap devices for electric vehicle systems[J].Scientific Reports, 2024, 14(1).DOI:10.1038/s41598-024-55426-6.
[15] He B. Failure mechanism analysis of IGBT based on Comsol multiphysics field coupling simulation[D]. Harbin Institute of Technology, 2021. DOI:10.27063/d.cnki.ghlgu.2021.000367.